Molecular Origins of the Slow Streptavidin−Biotin Dissociation Kinetics

Ashutosh Chilkoti and Patrick S. Stayton*

Contribution from the Center for Bioengineering, Box 357962, University of Washington, Seattle, Washington 98195

Received January 26, 1995[⊗]

Abstract: The association of streptavidin and avidin with biotin is among the strongest known noncovalent protein−ligand interactions ($K_a \approx 2.5 \times 10^{13}$ M^{-1}) and is controlled by an exceptionally slow off-rate. We have used this model system to elucidate the role of aromatic tryptophan side-chain binding contacts in the dissociation reaction coordinate and relatedly to the construction of the activation barrier and to the structure of the transition state. The significantly lower dissociation $t_{1/2}$ of conservative Trp to Phe site-directed mutants, 35 h (wild-type) > 5.5 h (W79F) > 2 h (W108F) > 0.5 h (W120F), reveals the importance of these Trp contacts in regulating the dissociation rate and also highlights the position dependence of the Trp contributions, most notably the optimized "capping" interaction of Trp 120 with biotin. We have also conducted a transition state analysis of the temperature-dependent dissociation kinetics, which along with the independent estimation of the equilibrium biotin-binding free energies and enthalpies has provided thermodynamic profiles defining the enthalpic, entropic, and free energy barriers to dissociation for the mutants relative to wild-type streptavidin. The increased biotin off-rate for W79F, which contacts the valeric acid moiety of biotin, and for W120F, which partially caps the bicyclic ring system, is caused largely by free energy destabilization of the ligand-bound ground state relative to wild-type streptavidin. This free energy destabilization is controlled by a 2.4 kcal mol^{-1} entropic destabilization of the ligand-bound W79F ground state relative to wild-type at 298 K, and a 5.1 kcal mol^{-1} enthalpic destabilization of the ligand-bound W120F ground state relative to wild-type. W79F displays an increased equilibrium binding enthalpy relative to wild-type, and thus streptavidin sacrifices potential binding enthalpy to minimize the entropic costs of biotin immobilization. This energetic role correlates well with the structural role of Trp 79, where the side chain contacts the valeric acid tail of biotin, the most conformationally flexible portion of the ligand and thus the most entropically costly to immobilize. The 17-fold increase in off-rate for W108F, on the other hand, which contacts the bicyclic ring of biotin from a buried position within the biotin-binding site, is largely due to the stabilization of the transition state, and is driven by a large 6.5 kcal mol^{-1} increase in the favorable activation entropy relative to wild-type streptavidin at 298 K. These results are consistent with a snapshot of the transition state where biotin and/or the protein have moved such that Trp 79 and Trp 120 no longer maintain strong contact with biotin, while the contact with Trp 108 remains energetically significant.

Introduction

The detailed molecular mechanisms by which proteins regulate small molecule recognition are of great fundamental and applied interest. Of particular importance to biology and the field of structure-based drug design are the biophysical processes governing tight-binding interactions.[1] In many respects, the dissociation reaction coordinate and off-rate is the key determinant of high-affinity interactions. This is because protein−small molecule on-rates typically fall within one order of magnitude of the diffusion limit, with an outer limit of two or three orders of magnitude, whereas the corresponding off-rates vary over a large range that can be conservatively estimated at 10^{12}. It is interesting to note, however, how little is known about this apparently straightforward and "simple" protein−ligand dissociation reaction coordinate. In contrast, a much clearer understanding of the protein folding transition state and reaction coordinate energetics has been gained by concerted site-directed mutagenesis and biophysical studies.[2] Similarly, a considerable body of knowledge exists on the enzyme-mediated reaction coordinate and the concurrent management of transition state energetics. On the other hand, the molecular nature of the transition state for protein−small molecule dissociation remains remarkably poorly characterized and understood in terms of structure and activation barrier relationships. From the perspective of slow dissociation kinetics, the problem for the protein is building a large activation barrier, the inverse of our classical picture of enzyme-mediated substrate catalysis. In addition, the protein must achieve this differential recognition of the ground state and transition state with a chemically invariant ligand, rather than with a structurally altered transition state substrate on its way to being converted to product.

As a starting point in efforts to elucidate how a large activation barrier to ligand dissociation is built, we have studied

* Author to whom correspondence should be addressed. Telephone: (206) 685-8148. FAX: (206) 685-8256.

⊗ Abstract published in *Advance ACS Abstracts*, October 1, 1995.

(1) (a) Meeting Abstract: Science Innovations '92, Protein Structure-based Rational Drug Design. *Science* **1992**, *258*, 36. (b) Weber, P. C.; Pantoliano, M. W.; Thompson, L. D. *Biochemistry* **1992**, *31*, 9350−9354. (c) Weber, P. C.; Pantoliano, M. W.; Simons, D. M.; Salemme, F. R. *J. Am. Chem. Soc.* **1994**, *116*, 2727−2724. (d) Weber, P. C.; Wendoloski, J. J.; Pantoliano, M. W.; Salemme, F. R. *J. Am. Chem. Soc.* **1992**, *114*, 3197−3200.

(2) (a) Otzen, D. E.; Itzhaki, L. S.; ElMasry, N. F.; Jackson, S. E.; Fersht, A. R. *Proc. Natl. Acad. Sci. U.S.A.* **1994**, *91*, 10422−10425. (b) Sancho, J.; Meiering, E. M.; Fersht, A. R. *J. Mol. Biol.* **1991**, 1007−1014. (c) Chen, X.; Matthews, C. R. *Biochemistry* **1994**, *33*, 6356−6362. (d) Alexander, P.; Orban, J.; Bryan, P. *Biochemistry* **1992**, *31*, 7243−7248.

(3) (a) Weber, P. C.; Ohlendorf, D. H.; Wendoloski, J. J.; Salemme, F. R. *Science* **1989**, *243*, 85−88. (b) Hendrickson, W. A.; Pahler, A.; Smith, J. L.; Satow, Y.; Meritt, E. A.; Phizackerley, R. P. *Proc. Natl. Acad. Sci. U.S.A.* **1989**, *86*, 2190−2194.

0002-7863/95/1517-10622$09.00/0

the high-affinity streptavidin−biotin model system. The exceptionally tight binding observed in the streptavidin/avidin interaction with biotin ($K_a = 10^{14}-10^{15}$ M^{-1})[9] is controlled by the slow dissociation kinetics of the protein−ligand complex,[10,11] in common with other high-affinity systems.[12] The X-ray crystal

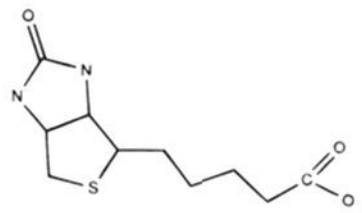

1

structure of the streptavidin tetramer complexed with biotin reveals an extensive set of hydrogen-bonding and van der Waals interactions between protein and ligand, and comparison with the biotin-free structure suggests that biotin association is also accompanied by the ordering of two surface loops.[3] These structural motifs have been observed in numerous protein−ligand systems,[4−6] and the involvement of aromatic side chains is particularly widespread in high-affinity complexes.[6] The elucidation of the structure−function relationships underlying the biotin dissociation kinetics is thus of broad interest as a paradigm for tight-binding protein−ligand interactions. Computational[7] and site-directed mutagenesis studies[8] have suggested that the large free energy decrease associated with biotin binding is largely attributable to hydrophobic and van der Waals interactions between biotin and four Trp residues in the binding site of streptavidin. Three Trp residues line the biotin-binding pocket, Trp 79, Trp 92, and Trp 108, while Trp 120 is contributed by an adjacent dyad-related subunit.

We investigate here the molecular origins of the slow biotin off-rate with concerted site-directed mutagenesis and biophysical studies of the ligand reaction coordinate. We have probed the structural and energetic contributions of three key aromatic binding contacts to both the transition state and the protein−ligand complex, with conservative alterations of tryptophan side chains to phenylalanine (Figure 1). A complete set of equilibrium and activation thermodynamic parameters for wild-type streptavidin

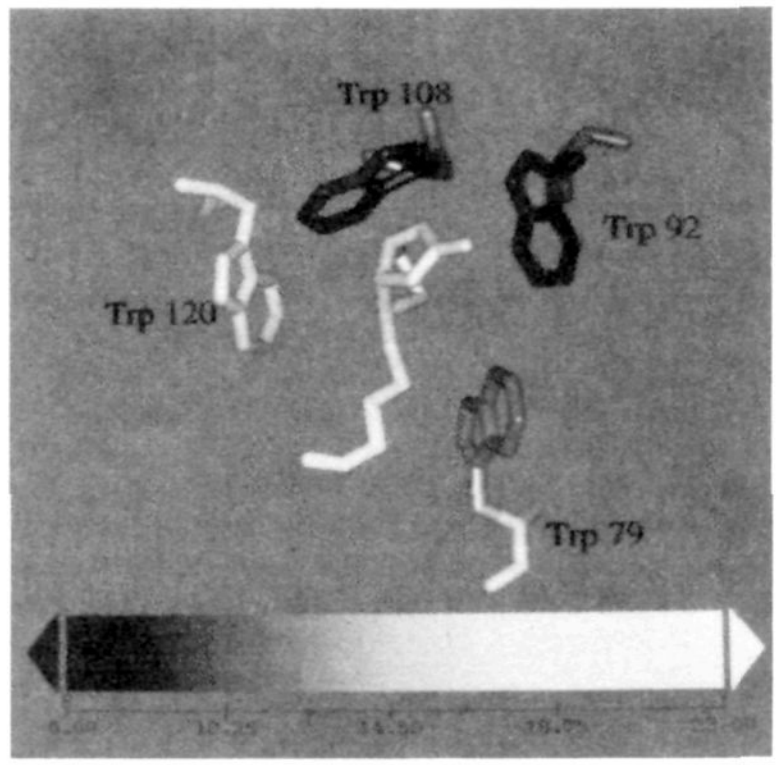

Figure 1. The aromatic binding-site contacts of streptavidin with biotin, showing the spatial relationships between biotin, Trp 79, Trp 92, Trp 108, and Trp 120. Atoms are gray-scaled according to the spectrum-scaled crystallographic B-factors, from black at low values to white at the higher end of this scale.

and the mutants has provided a map of differential transition state interactions with biotin relative to the ground state, and thus a partial structural model of the transition state. Relatedly, kinetic and thermodynamic characterization of the site-directed mutants has provided considerable mechanistic insight into the dissociation reaction coordinate through the interpretation of the enthalpic and entropic contributions to the activation barrier.

Experimental Section

Protein Expression. The design and mutagenesis of the recombinant core streptavidin gene, its expression in a T7 expression system (pET-21a, Novagen, Inc., Madison, WI), and the isolation, refolding, purification, and structural and preliminary functional characterization of WT streptavidin and the Trp-to-Phe site-directed mutants have been reported previously.[8]

Streptavidin−Biotin Dissociation Kinetics. 8,9-^{3}H biotin (4.8 μL, 21 μM, NEN/Dupont) was added to 10 mL of PBS, pH 7.4, 1 mM EDTA, containing WT streptavidin or one of the mutants W79F, W108F, or W120F at a concentration of 0.5 μM and incubated for 10 min followed by addition of nonradioactive biotin (20 mM) to a final concentration of 50 μM. Aliquots (0.5 mL) of this mixture were centrifugally ultrafiltered through a 30 000 MW cutoff filter (Microcon-30, Amicon Inc., Berverly, MA) to separate the unbound biotin from the protein−ligand complex. Fifty microliters of the filtrate was mixed with 10 mL of scintillation cocktail in triplicate and assayed for radioactivity in a liquid scintillation counter (LS-7000, Beckman Instruments, Fullerton, CA). The average radioactivity of the filtrate in cpm at each time point (x) and radioactivity of the protein−ligand complex before addition of cold biotin (a) allowed the first-order rate constant of the dissociation of the protein−ligand complex (k_{off}) to be determined from the plot of $\ln(a - x/a)$[ln(fraction bound)]. Error bars indicate the standard deviation associated with three independent measurements. Control experiments where no cold biotin was added yielded <2% of the total radioactivity in the ultrafiltrate, demonstrating that all ^{3}H biotin is initially bound.

Activation Thermodynamic Parameters. The dissociation kinetics of the biotin−protein complex were determined as described above at temperatures ranging from 10 to 35 °C. Since WT streptavidin and mutants are stable in this temperature range, the temperature dependence of the dissociation rate is assumed to be kinetically related. The activation thermodynamic parameters, $\Delta G_r^{\ddagger}$, $\Delta H_r^{\ddagger}$, and $\Delta S_r^{\ddagger}$, were determined by transition state analysis of the dependence of the dissociation

(4) (a) Krebs, J. F.; Ippolito, J. A.; Christianson, D. W.; Fierke, C. A. *J. Biol. Chem.* **1993**, *268*, 27458−27466. (b) Yano, T.; Mizuno, T.; Kagamiyama, H. *Biochemistry* **1993**, *32*, 1810−1815. (c) Heinz, D. W.; Hyberts, S. G.; Peng, J. W.; Priestle, J. P.; Wagner, G.; Grutter, M. G. *Biochemistry* **1992**, *31*, 8755−8766. (d) Matsumara, M.; Fremont, D. H.; Peterson, P. A.; Wilson, I. A. *Science* **1992**, *257*, 927−934.

(5) (a) Falzone, C. J.; Wright, P. E.; Benkovic, S. J. *Biochemistry* **1994**, *33*, 439−442. (b) Noble, M. E.; Zeelen, J. P.; Wierenga, R. K. *Proteins* **1993**, *16*, 311−326. (c) Gekko, K.; Yamagami, K.; Kunori, Y.; Ichihara, S.; Kodama, M.; Iwakura, M. *J. Biochem. (Tokyo)* **1993**, *113*, 74−80. (d) Kempner, E. S. *FEBS Lett.* **1993**, *326*, 4−10. (e) Yang, X. J.; Miles, E. W. *J. Biol. Chem.* **1992**, *267*, 7520−7528. (f) Wierenga, R. K.; Noble, M. E.; Postma, J. P.; Groendijk, H.; Kalk, K. H.; Hol, W. G.; Opperdoes, F. R. *Proteins* **1991**, *10*, 33−49. (g) Sampson, N. S.; Knowles, J. R. *Biochemistry* **1992**, *31*, 8488−8494. (h) Sampson, N. S.; Knowles, J. R. *Biochemistry* **1992**, *31*, 8482−8487.

(6) (a) Ronco, L. V.; Silverman, S. L.; Wong, S. G.; Slamon, D. J.; Park, L.; Gasson, J. C. *J. Biol. Chem.* **1994**, *269*, 277−283. (b) Bibbins, K. B.; Bouef, H.; Varmus, H. E. *Mol. Cell. Biol.* **1993**, *13*, 7278−7287. (c) Faurobert, E.; Otto-Bruc, A.; Chardin, P.; Chabre, M. *EMBO J.* **1993**, *12*, 4191−4198. (d) Bossard, M. J.; Koser, P. L.; Brandt, M.; Bergsma, D. J.; Levy, M. A. *Biochem. Biophys. Res. Commun.* **1991**, *176*, 1142−1148. (e) Padlan, E. A.; Silverton, E. W.; Sheriff, S.; Cohen, G. H.; Smith-Gill, S. J.; Davies, D. R. *Proc. Natl. Acad. Sci. U.S.A.* **1989**, *86*, 5938−5942. (f) Anglister, J.; Levy, R.; Scherf, T. *Biochemistry* **1989**, *28*, 3360−3365.

(7) (a) Miyamoto, S.; Kollman, P. *Proteins* **1993**, *16*, 226−245. (b) Miyamoto, S.; Kollman, P. *Proc. Natl. Acad. Sci. U.S.A.* **1993**, *90*, 8402−8406.

(8) Chilkoti, A.; Tan, P. H.; Stayton, P. S. *Proc. Natl. Acad. Sci. U.S.A.* **1995**, *92*, 1754−1758.

(9) Green, N. M. *Adv. Protein Chem.* **1975**, *29*, 85−143.

(10) Green, N. M. *Biochem. J.* **1963**, *89*, 585−591.

(11) Piran, U.; Riordan, W. J. *J. Immunol. Methods* **1990**, *133*, 141−143.

(12) Smith, T. W.; Kubitz, K. M. *Biochemistry* **1975**, *14*, 1496−1502.

rate constant upon temperature, which is described by the Eyring equation:[13]

$$k_{off} = \frac{k_B T}{h} \exp(-\Delta G_r^{\ddagger}/RT) \quad (1)$$

where k_B, h, and R are the Boltzmann, Planck, and universal gas constants, $\Delta G_r^{\ddagger}$ is the activation energy of dissociation of the protein–ligand complex, and T is the absolute temperature. The enthalpy is assumed to be temperature independent in the temperature range studied here. Furthermore, the transmission coefficient κ (not shown) on the right-hand side of eq 1 has been assumed to be unity. The activation enthalpy and entropy can be determined by partitioning $\Delta G_r^{\ddagger} = \Delta H_r^{\ddagger} - T\Delta S_r^{\ddagger}$ into a linearized form of eq 1:

$$\ln(k_{off}/T) = -\Delta H_r^{\ddagger}/R(1/T) + \text{constant} \quad (2)$$

A linear least-squares fit of a plot of $\ln(k_{off}/T)$ versus $1/T$ provided the activation enthalpy ($\Delta H_r^{\ddagger}$) and entropy of activation ($\Delta S_r^{\ddagger}$).

Isothermal Titration Calorimetry. Isothermal titration calorimetry (ITC) was performed using a MicroCal Omega titration calorimeter (Northampton, MA).[14] Streptavidin solutions ranging in concentration from 13 to 18 μM (cell volume 1.3625 mL) at 25 °C (the precise temperatures are reported in Table 3) were titrated by addition of 12 × 15 μL aliquots of biotin (0.25 mM) dissolved in the same buffer as the protein. The amount of power required to maintain the cell at constant temperature was monitored as a function of time. Preliminary experiments performed in buffers with different heats of ionization to determine the contribution, if any, of protonation to the measured equilibrium binding enthalpy yielded identical binding enthalpies within experimental error, indicating the absence of any such contribution. The experiments reported here were performed in 50 mM Tris·HCl, 50 mM NaCl, pH 8.0. Ligand concentrations were determined gravimetrically: typically, a 15 mM biotin stock in the titration buffer was prepared by dissolution of the required amount of biotin in buffer and diluted to 0.25 mM for a set of experiments. WT streptavidin concentrations were determined by optical absorbance at 280 nm using the subunit extinction coefficient of 34 000 M^{-1} cm^{-1}.[15] Concentrations of the Trp to Phe mutants were also determined by optical absorbance, using ϵ_{280} for WT streptavidin corrected by the method of Gill and vonHippel for the Trp to Phe substitution.[16] These concentrations showed agreement to within 5% with those obtained by fluorescence titration with fluorescein–biotin.[17]

The data were analyzed with software developed at the Biocalorimetry Center (Johns Hopkins University, Baltimore, MD) by determination of the observed reaction heat for each titration step. The heats of dilution for each ligand injection, which were less than 5% of the binding enthalpies, were subtracted from the reaction heat. Nonlinear least-squares fitting of the corrected reaction heat allowed the binding stoichiometry (n) and equilibrium binding enthalpy ($\Delta H°$) to be determined, assuming one set of sites with no cooperativity between subunits of the tetrameric streptavidin.[18] The $\Delta H°$ values so determined were compared to those obtained from the corrected reaction heat under conditions of complete binding of ligand (i.e., the first few ligand injections) and the amount of ligand injected and were found to agree within 0.2 kcal mol^{-1}.

Equilibrium Biotin-Binding Free Energies. The ΔK_d values for biotin binding by WT streptavidin and mutants were estimated by linear least-squares fitting of the linearized ELISA binding isotherms with iminobiotin as the ligand[8] by the method of Lilliom et al.:[19]

$$1/(1 - i) = (p/K_d)(C_0/i) - (F/V)(q/K_d)L \quad (3)$$

where C_0 = bulk concentration of protein in microtiter wells, i = normalized absorbance values = absorbance (405 nm)/absorbance (405 nm)$_{max}$, K_d = equilibrium dissociation constant, F = reaction area in the microtiter well, V = reaction volume, L = surface concentration of the ligand, p = number of occupied binding sites per protein molecule, and q = total number of ligand binding sites per protein molecule. A plot of $1/1 - i$ versus C_0/i should give a straight line and the apparent dissociation constant $K_d^{app} = K_d/p$. If p is known, the absolute value of the dissociation constant can be determined. In the present case, we have determined K_d^{app} for the binding of 2-iminobiotin to WT streptavidin and the Trp to Phe mutants and assumed p to be invariant in every experiment, which then allows ΔK_d to be determined as K_d(mutant)/K_d(WT). At least three independent sets of binding isotherms for each streptavidin variant were analyzed to determine individual K_d^{app}. The K_d^{app} for WT streptavidin, which was included in each set as an internal control, was used to determine the ΔK_d for individual mutants in each set. The individual ΔK_d for each mutant were then averaged to yield the ΔK_d values for the streptavidin mutants as well as the standard deviations, reported in Table 1.

Table 1. The Rate Constant for the Dissociation of Biotin–Protein Complex k_{off} (s^{-1}),[a] Relative Dissociation Rate Constant Δk_{off}, Relative Equilibrium Dissociation Constant ΔK_d,[a] and $\Delta\Delta G°$ (kcal mol^{-1}) for WT Streptavidin and W79F, W108F, and W120F Mutants at 298 K

protein	k_{off} (s^{-1})	Δk_{off}[b]	ΔK_d[a]	$\Delta\Delta G°$[d]
WT	5.4×10^{-6}	1	1	0
W79F	3.6×10^{-5}	5.5	4.4 ± 1.8	+0.9
W108F	9.6×10^{-5}	17	2.9 ± 1.0	+0.6
W120F	3.7×10^{-4}	70	50.4 ± 7.7	+2.3

[a] Δk_{off} and ΔK_d are defined relative to WT streptavidin. [b] $\Delta k_{off} = k_{off}$(mutant)/k_{off}(WT). [c] $\Delta K_d = K_d$(mutant)/K_d(WT). [d] $\Delta\Delta G° = RT \ln(\Delta K_d)$.

Results

Biotin-bound recombinant core wild-type (WT) streptavidin and the conservative site-directed mutants W79F, W108F, and W120F display monoexponential, first-order, dissociation kinetics (Figure 2). The first-order dissociation rate constants (k_{off}) are summarized in Table 1. The k_{off} of recombinant core WT streptavidin reported here ($k_{off} = 5.6 \times 10^{-6}$ s^{-1}) is approximately twice that reported earlier for a commercial preparation of streptavidin,[11] although we note that we obtain monophasic dissociation kinetics for recombinant core WT streptavidin, as compared to the multiphase kinetics observed with commercial preparations of streptavidin which complicate the rate determination.

The effects of replacing the Trp residues in contact with biotin by Phe are significant and position-dependent. There is a large effect on the k_{off} upon replacing Trp 120 with Phe: the conservative W120F mutation results in a 70-fold increase in the dissociation rate constant, relative to WT streptavidin, corresponding to a decrease in the $t_{1/2}$ from 35 (WT) to 0.5 h (W120F). The effects of replacing Trp with Phe at positions 79 and 108 are also significant, though smaller in magnitude. The k_{off} for W79F is 5-fold greater and that of W108F is 17-fold greater than WT streptavidin. The Δk_{off} of W79F and W120F relative to WT streptavidin, summarized in Table 1, are similar in magnitude to their ΔK_d, suggesting that the decreased equilibrium affinity of W79F and W120F can be largely accounted for by their increased k_{off}. W108F, on the other hand, displays a biotin Δk_{off} that is larger than the ΔK_d, suggesting that corresponding on-rate alterations also exist. The W108F on-rate remains close to the diffusion limit, given the

(13) (a) Evans, M. G.; Polanyi, M. *Trans. Faraday Soc.* **1935**, *31*, 875–894. (b) Eyring, H. *J. Chem. Phys.* **1935**, *3*, 107–115.

(14) (a) Wiseman, T.; Williston, S.; Brandts, J. F.; Lin, L. N. *Anal. Biochem.* **1989**, *179*, 131–137. (b) Freire, E.; Mayorga, O. L.; Straume, M. *Anal. Chem.* **1989**, *62*, 950A–959A.

(15) Sano, T.; Cantor, C. R. *Proc. Natl. Acad. Sci. U.S.A.* **1990**, *87*, 142–146.

(16) Gill, S. C.; von Hippel, P. H. *Anal. Biochem.* **1989**, *182*, 319–326.

(17) Chilkoti, A.; Stayton, P. S. Unpublished results.

(18) For ligand binding to n independent sites, non-linear least-squares fitting of the heat of reaction as a function of the ligand concentration yields the number of binding sites (n), the equilibrium ligand binding enthalpy ($\Delta H°$), and the equilibrium dissociation constant (K_d) when MK_a (M is the total protein or macromolecule concentration in the cell and $K_a = 1/K_d$) is between 10 and 100. In this case the K_a is $\geq 10^7$ M^{-1} in all cases, and M is $\sim 15 \times 10^{-6}$ M; thus $MK_a > 100$ in all cases, and the values of K_a obtained from the fit are not reliable.

(19) Lilliom, K.; Orosz, F.; Horvath, L.; Ovadi, L. *J. Immunol. Methods* **1991**, *143*, 119–125.

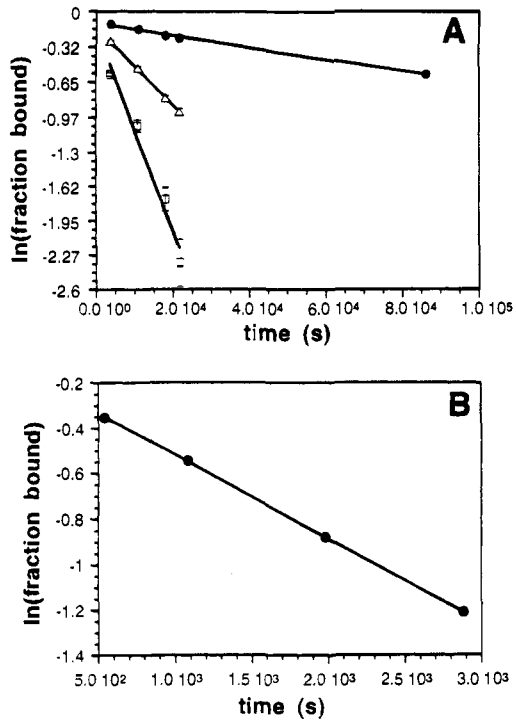

Figure 2. Streptavidin–biotin dissociation rate at 298 K: (a) WT streptavidin (filled circle), W79F (open triangle), and W108F (open square); (b) W120F (filled circle).

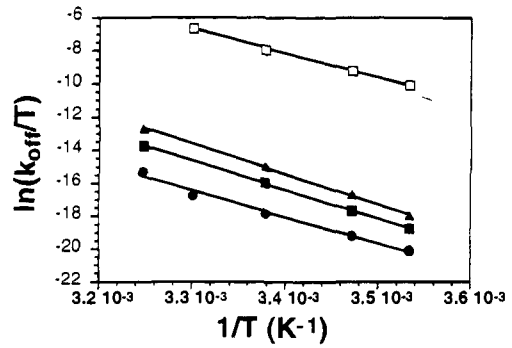

Figure 3. Eyring plots for the dissociation of the streptavidin–biotin complex. Lines are theoretical fits according to eq 2: (filled circles) WT streptavidin, (filled squares) W79F, (filled triangles) W108F, and (open squares) W120F.

experimental uncertainty in the biotin-binding K_d reported by Green.[9] These results suggest that the alterations in the off-rate kinetics for W79F and W120F are largely accounted for by a free energy destabilization of the ligand-bound ground state relative to WT streptavidin, while stabilization of the transition state of W108F relative to WT largely accounts for the Δk_{off} of this mutant.

The energetic origins of the marked differences in k_{off} for W79F, W108F, and W120F were further examined by measuring the temperature dependence of the dissociation rates and applying transition state theory to determine the enthalpic and entropic contributions to the activation barrier.[13] Eyring plots of the off-rate constants as a function of temperature are shown in Figure 3. The activation thermodynamic parameters are summarized in Table 2, calculated with the assumption of a single averaged transition state by a least-squares fit of the data shown in Figure 3 and the use of eq 2.[20] The slow biotin off-rate is due to a large activation barrier, $\Delta G_r^{\ddagger} = 24.4$ kcal mol^{-1},

(20) The $\Delta\Delta G_r^{\ddagger}$ values determined from transition state theory analysis of the data ($\Delta\Delta G_r^{\ddagger} = \Delta\Delta H_r^{\ddagger} - T\Delta S_r^{\ddagger}$) are identical to the values calculated from the k_{off} at 298 K ($\Delta\Delta G_r^{\ddagger} = -RT \ln[k_{off}(\text{mutant})/k_{off}(\text{WT})]$, thus providing an internal check on the validity of this analysis.

Table 2. Thermodynamic Parameters Derived from Transition State Analysis of the Temperature-Dependent Dissociation of the Biotin–Streptavidin (WT or mutant) Complex[a]

protein	$\Delta H_r^{\ddagger}$	$T\Delta S_r^{\ddagger}$ [b]	$\Delta G_r^{\ddagger}$ [c]	$\Delta\Delta G_r^{\ddagger}$ [d]
WT	32 ± 2.1	7.6 ± 2.1	24.4 ± 2.4	0
W79F	34.9 ± 0.6	11.6 ± 0.6	23.3 ± 0.8	−1.1
W108F	36.5 ± 0.9	13.8 ± 0.9	22.7 ± 1.3	−1.7
W120F	28.5 ± 1.0	6.6 ± 1.0	21.9 ± 1.4	−2.5

[a] All values are in kcal mol^{-1}. [b] $T = 298$ K. [c] $\Delta G_r^{\ddagger} = \Delta H_r^{\ddagger} - T\delta S_r^{\ddagger}$. [d] $\Delta\Delta G_r^{\ddagger} = \Delta G_r^{\ddagger}(\text{mutant}) - \Delta G_r^{\ddagger}(\text{WT})$.

Table 3. Equilibrium Biotin-Binding Enthalpies (kcal mol^{-1}) of WT Streptavidin and Trp to Phe Mutants Measured by Isothermal Titration Calorimetry

protein	T^a	n^b	ΔH° [c]	$\Delta\Delta H^{\circ}$ [d]
WT	25.0	0.97	−24.5	0
W79F	25.3	0.86	−26.0 ± 0.5[e]	−1.5 ± 0.7
W108F	25.2	0.88	−23.5	+1.0 ± 0.7
W120F	25.0	0.9	−19.4	+5.1 ± 0.7

[a] Temperature (T) in °C. [b] n and ΔH° were obtained from a nonlinear least-squares fit of the calorimetric binding isotherm; details are in the text. [c] The ΔH° values reported here were compared with those obtained directly from the corrected reaction heat and the moles of ligand injected under conditions where all of the ligand injected is bound (i.e., the first few injections) and were found to agree within 0.2 kcal mol^{-1}. Similarly, comparison of the values reported in the table with ΔH° calculated using total protein present in the calorimeter cell yielded values within 5% of those reported in the table. We note that the errors in the ΔH° values reported are ~5%, and largely arise from errors in the determination (gravimetric) of ligand concentration and protein concentration (optical absorbance at 280 nm). [d] $\Delta\Delta H = \Delta H^{\circ}_{\text{mutant}} - \Delta H^{\circ}_{\text{WT}}$. [e] Average of two independent experiments.

for biotin dissociation. The activation barrier is enthalpic in origin, $\Delta H_r^{\ddagger} = +32$ kcal mol^{-1}, with a positive activation entropy of 7.6 kcal mol^{-1} at 298 K. An unexpected finding is that both W79F and W108F exhibit a larger activation enthalpy of dissociation (+2.9, +4.5 kcal mol^{-1}) compared to WT streptavidin. However, the Trp to Phe substitution results in an even larger positive increase in the activation entropy contribution, as the $T\Delta S_r^{\ddagger}$ term for W79F and W108F favors dissociation relative to WT streptavidin by 4–6 kcal mol^{-1} at 298 K. In direct contrast, the 70-fold faster off-rate of W120F (corresponding to a $\Delta\Delta G_r^{\ddagger}$ of −2.1 kcal mol^{-1} relative to WT streptavidin) largely arises from a decreased activation enthalpic barrier ($\Delta H_r^{\ddagger} = +28.5$ kcal mol^{-1}), with an activation entropy that is very similar to that of WT streptavidin.

The determination of $\Delta G_r^{\ddagger}$ by transition state analysis and the independent estimation of ΔG° from affinity measurements allows the determination of free energy profiles for WT streptavidin and the Trp to Phe mutants. Similarly, the enthalpic energy profiles can be drawn from the equilibrium biotin-binding enthalpy (ΔH°), independently determined by isothermal titration calorimetry measurements (results are summarized in Table 3), and $\Delta H_r^{\ddagger}$ available from transition state analysis of the temperature-dependent protein-ligand dissociation kinetics. This analysis allows the free energy barriers responsible for the off-rates of the different mutants to be delineated in terms of alterations in the transition state and/or the biotin-bound ground state, and further partitions these free energy changes into enthalpic and entropic components. Upon comparison with the results for WT streptavidin, the thermodynamic effects of mutating specific residues can be mapped, providing considerable insight into the structure and energetics of the transition state.

The free energy profiles for WT streptavidin and the Trp to Phe mutants are shown in Figure 4a and the data utilized to construct these profiles are summarized in Table 4. The 70-fold decrease in the k_{off} of W120F is due to the destabilization of its biotin-bound ground state relative to WT streptavidin. $\Delta\Delta G^{\circ} = +2.3$ kcal mol^{-1} vs $\Delta\Delta G_r^{\ddagger} = -2.5$ kcal mol^{-1}. This

Table 4. Summary of Biotin-Binding Equilibrium Thermodynamic Difference Parameters (kcal mol^{-1}) and Activation Thermodynamic Difference Parameters of Streptavidin–Biotin Dissociation for WT Streptavidin and Trp Site-Directed Mutants at 298 K[a]

protein	$\Delta\Delta G°$	$\Delta\Delta H°$	$\Delta\Delta G_r^‡$	$\Delta\Delta H_r^‡$
WT	$\Delta G° = -18.3$	$\Delta H° = -24.5 \pm 0.5$	$\Delta G_r^‡ = 24.4 \pm 2.4$	$\Delta H_r^‡ = 32 \pm 2.1$
streptavidin	$\Delta\Delta G° = 0$	$\Delta\Delta H° = 0$	$\Delta\Delta G_r^‡ = 0$	$\Delta\Delta H_r^‡ = 0$
W79F	0.8	−1.5	−1.1	+2.9
W108F	0.5	+1.0	−1.7	+4.5
W120F	2.7	+5.1	−2.5	−3.5

[a] All thermodynamic parameters are in kcal mol^{-1}.

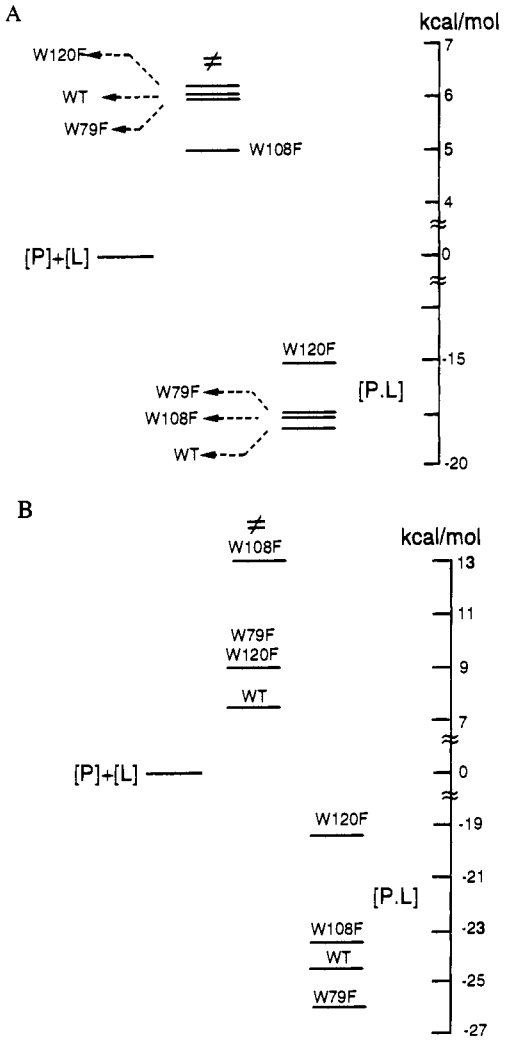

Figure 4. Thermodynamic profiles for WT streptavidin and W79F, W108F, and W120F: (a) Gibbs free energy (ΔG); (b) enthalpy (ΔH). Free energies and enthalpies of the biotin-bound mutants and WT streptavidin [P.L.] are shown with reference to the unbound protein [P] and free ligand [L]. It is assumed that these structural alterations are thermodynamically non-disruptive, *i.e.*, do not alter the reference level of the mutants in the ligand free state with respect to WT streptavidin. The biotin-bound complex is defined using the $\Delta G°$ and $\Delta H°$ values in Tables 2 and 3, respectively. The transition state ($\neq$) of WT streptavidin and the Trp to Phe mutants is defined with respect to the position of the respective ligand-bound complex using the $\Delta H_r^‡$ and $\Delta G_r^‡$ values in Table 2.

alteration in the free energy of the ligand-bound state upon mutating Trp 120 to Phe is enthalpically controlled, $\Delta\Delta H° = +5.1$ kcal mol^{-1}, with a favorable entropy term, $T\Delta S° = +2.8$ kcal mol^{-1} (Figure 4b). W79F displays the smallest decrease in the k_{off}, which can also be attributed to the destabilization of the biotin-bound ground state. The origin of this +0.9 kcal mol^{-1} $\Delta\Delta G°$ term is interesting and notably different than W120F. The change in equilibrium binding enthalpy actually favors association since $\Delta\Delta H° = -1.5$ kcal mol^{-1}, indicating that the free energy destabilization of the biotin-bound state caused by mutating Trp 79 to Phe is caused by an even larger unfavorable entropic alteration, $T\Delta S° = -2.4$ kcal mol^{-1}.

A key finding from the thermodynamic profiles of these mutants is the role of Trp 108 in destabilizing the transition state. We note that the thermodynamic effects ensuing from mutating Trp 79 and Trp 120 to Phe are largely reflected in free energy alterations in the biotin-bound ground state, with little effect on the transition state (Figure 4a). W108F is notably different, as the stabilization of the transition state by the Trp to Phe alteration accounts for 1.1 kcal mol^{-1} of the total 1.7 kcal mol^{-1} reduction in the activation barrier. The transition state analysis suggests that the stabilization is entropically controlled, $T\Delta S_r^‡ = +6.2$ kcal mol^{-1} relative to wild-type, but there is also a large compensating enthalpic destabilization of the transition state, $\Delta\Delta H_r^‡ = +4.5$ kcal mol^{-1}. These large alterations strongly imply a critical role for Trp 108 in the transition state complex as further discussed in the following section.

Discussion

The streptavidin–biotin complex is characterized by three motifs found either individually or collectively in many tight-binding systems—an extensive hydrogen bonding network,[4] prominent aromatic side-chain contacts,[6] and flexible loop closure associated with ligand binding.[5] The exceptionally slow biotin off-rate that defines the binding equilibrium is similarly a common feature of many high-affinity systems. Insight into the molecular mechanisms controlling the slow dissociation kinetics should thus be of general significance to many important biological systems, and specifically to the field of structure-based drug design where these features generally represent the target goals for therapeutic development. While site-directed mutagenesis approaches have provided considerable insight into the mechanisms by which enzymes control the catalytic activation barriers associated with substrate turnover, there has been remarkably little dissection of the activation barriers governing ligand dissociation kinetics. Whereas enzymes utilize binding energy to minimize the free energy of the transition state, a high barrier to ligand dissociation implies that the protein maximizes the free energy of the transition state. A key question is how this large activation barrier can be built when the ligand remains chemically unaltered in the transition state. In contrast, the differential binding energy in enzyme-mediated catalysis can often be directly related to the altered structure of the substrate in the transition state relative to the ground state.

In structural and energetic terms, this challenge can most obviously be met by controlling the activation barrier through a combination of protein/ligand conformational changes (including changes in conformational entropy) and related differential transition state binding interactions. Indeed, kinetically important protein conformational changes associated with ligand dissociation have been described in several systems.[21] In our model, we only consider the lowest free energy level corresponding to the bound state and an averaged highest free energy level on the dissociation reaction coordinate, i.e. the transition state, with a reference free energy state of the free protein and

ligand in solution, assumed to be identical for wild-type and the mutants. We thus do not discriminate between potentially separable conformational changes and the microscopic dissociation rate process, as we do not have experimental evidence validating such a treatment. We will thus refer to degenerate protein and/or ligand changes to reflect transition state structural alterations. While this model appears to provide considerable insight into the structure and energetics of the transition state, its limitations should be borne in mind.

Structure of the Transition State. The thermodynamic profiles map the relative structural contributions of Trp 79, 108, and 120 to the ground state and transition state. The alteration in the activation free energy is largely equivalent to equilibrium alterations at positions 79 and 120, suggesting that these residues preferentially stabilize the bound ground state. Trp 108, on the other hand, is an important transition state contact, as the Phe mutant displays significant alterations of the transition state energy level rather than the ground state ($\Delta H^{TS} = +5.5$ kcal mol^{-1} and $T\Delta S^{TS} = +6.7$ kcal mol^{-1}). These results are thus consistent with a transition state model where Trp 108 maintains a significant binding contact with biotin in the transition state, while protein/ligand movement and structural alterations have greatly weakened the Trp 79 and Trp 120 interactions (Figure 5). Our results suggest that the loop containing Trp 120 opens away from biotin, while the biotin and/or protein also shifts such that the valeric acid tail interacts less strongly with Trp 79. This sequence would be reversed on the biotin association reaction coordinate, and the enthalpic closure of the binding pocket would occur at some point after the transition state through the "capping" movement of Trp 120. We note that fluorescence dynamics studies of biotin binding by streptavidin provide complementary evidence supporting this structural scenario.[24]

It is interesting to compare the crystallographic *B* factors for these three tryptophan side chains in the biotin-bound state. The *B* factors for the Trp 108 side-chain atoms range from 8.5 to 13, while those for Trp 79 and Trp 120 range from 12.7 to 19 and 17 to 20, respectively (Figure 1). Crystallographic *B* factors have been commonly correlated with mobility[23] and the relatively high *B* factors for Trp 79 and Trp 120 in the bound state are thus consistent with the need for structural alterations at these positions in order to open the binding pocket and minimize transition state contacts. It is also important to note that the Trp 108 and Trp 92 indole nitrogens are internally hydrogen bonded in the bound and unbound states, thus immobilizing these side chains and explaining their low *B* factors. As the Phe side chains cannot form these anchoring contacts, an important source of the energetic differences between WT and the Phe mutant at position 108 could be related to the differential conformational entropy associated with side-chain anchoring. A larger loss in conformational entropy would be expected if the side chain is not anchored but becomes more ordered with biotin association, and this is observed with the W108F mutant in the transition state.

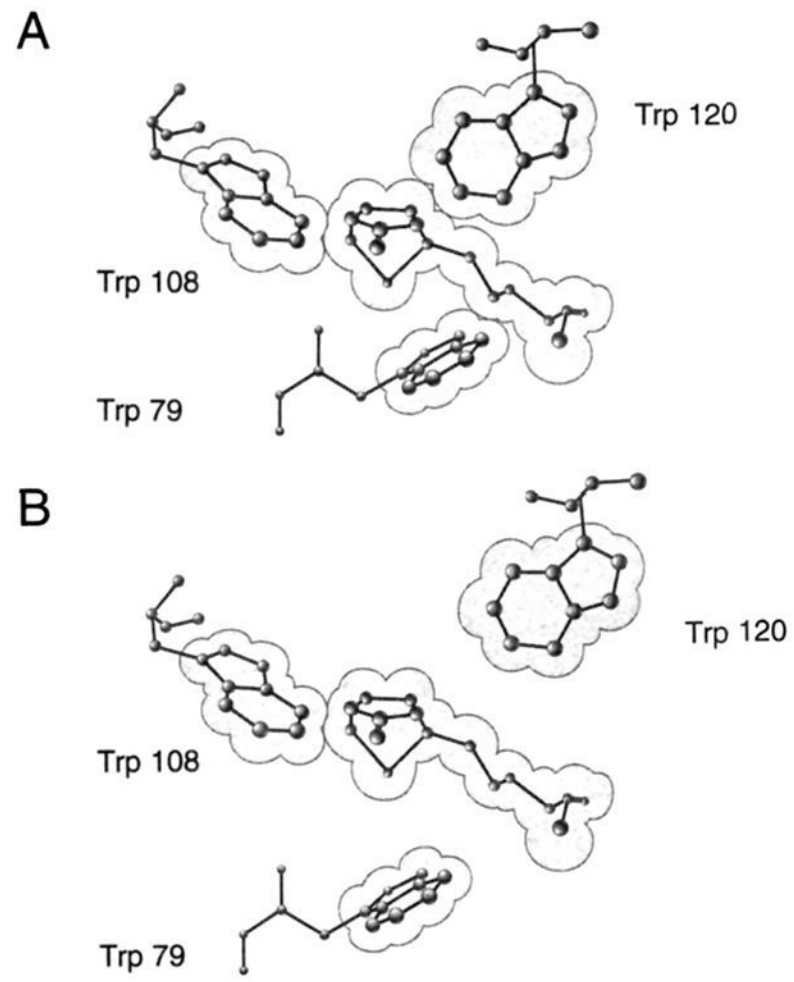

Figure 5. A schematic of the structural changes accompanying the formation of the transition state on the dissociation pathway of the streptavidin−biotin complex. (a) Ligand-bound ground state: Trp 79, 108, and 120 have substantial van der Waals/hydrophobic contact with biotin in the protein−ligand complex ground state. (b) Transition state: The formation of the transition state is marked by substantial loss of contact between biotin and Trp 79 and Trp 120. In contrast, Trp 108 retains substantial contact with biotin in the transition state.

Mechanistic Interpretation of the Activation Thermodynamic Parameters. The activation thermodynamic parameters indicate that the activation barrer to biotin dissociation is enthalpically dominated, suggesting that a number of protein−ligand binding contacts present in the ligand-bound state are severely weakened or broken in the transition state. As described above, our work suggests that Trp 120 and Trp 79 ground state contacts are greatly weakened in the transition state. In addition, biotin forms numerous H bonds with streptavidin side chains in the binding pocket in the biotin-bound ground state,[3] and the loss of these contacts in the transition state could also account for a significant fraction of the activation enthalpy of dissociation. The conformational changes associated with the loss of binding contacts and the opening of the binding pocket in the transition state would also be expected to be endothermic and thus to contribute significantly to the exceptionally large enthalpic activation barrier. The activation entropy for biotin dissociation is positive ($T\Delta S_r^{\ddagger} = +7.6$ kcal mol^{-1} at 298 K) and reveals that the formation of the transition state is entropically favored. This implies a greater degree of conformational entropy in the protein−ligand transition state relative to the ligand-bound ground state, arising from decreased binding interactions and subsequent increases in the mobility of the ligand and/or protein. The surface loop comprised of residues 45−50 that undergoes an order-to-disorder transition upon biotin dissociation[3] could also provide a substantial portion of this positive activation entropy if the disordering of this loop occurs in the transition state.

(21) (a) Edmundson, A. B.; Ely, K. R.; He, X. M.; Herron, J. N. *Mol. Immunol.* **1989**, *26*, 207−220. (b) Hansen, J. C.; Gorski, J. *J. Biol. Chem.* **1986**, *261*, 13990−13996. (c) Steitz, T. A.; Harrison, R.; Weber, I. T.; Leahy, M. *Ciba Found. Symp.* **1982**, *93*, 25−46. (d) Kranz, D. M.; Herron, J. N.; Voss, E. W., Jr. *J. Biol. Chem.* **1982**, *257*, 6987−6995. (e) Eftink, M. R.; Anuseim, A. C.; Biltonen, R. L. *Biochemistry* **1983**, *22*, 3884−3896. (f) Schimerlik, M. I.; Searles, R. P. *Biochemistry* **1980**, *19*, 3407−3413. (g) Chapuis-Cellier, C.; Gianizza, E.; Arnaud, P. *Biochim. Biophys. Acta* **1982**, *709*, 353−357.

(22) (a) Lumry, R.; Rajender, S. *Biopolymers* **1970**, *9*, 1125−1227. (b) Mukkur, T. K. *CRC Crit. Rev. Biochem.* **1984**, *16*, 133−167. (c) Zidovetski, R.; Blatt, Y.; Schepers, G.; Pecht, I. *Mol. Immunol.* **1988**, *25*, 379−383. (d) Murakami, K.; Sano, T.; Tsuchie, S.; Yasunaga, T. *Biophys. Chem.* **1985**, *21*, 127−136. (e) Jelesarov, I.; Bosshard, H. R. *Biochemistry* **1994**, *33*, 13321−13328. (f) Lee, B. *Biophys. Chem.* **1994**, *51*, 271−277. (g) Hu, D. D.; Eftink, M. R. *Biophys. Chem.* **1994**, *49*, 233−239. (h) Hibbits, K. A.; Gill, D. S.; Wilson, R. C. *Biochemistry* **1994**, *33*, 3584−3590. (i) Kuroki, R.; Nitta, K.; Yutani, K. *J. Biol. Chem.* **1992**, *267*, 24297−24301.

(23) Noble, M. E.; Wierenga, R. K.; Lambeir, A. M.; Opperdoes, F. R.; Thunissen, A. M. W. H.; Kalk, K. H.; Groendijk, H.; Hol, W. G. J. *Proteins* **1991**, *10*, 50−69.

(24) Kurzban, G. P.; Gitlin, G.; Bayer, E. A.; Wilchek, M.; Horowitz, P. M. *J. Protein Chem.* **1990**, *9*, 673−682.

The question of whether the transition state complex is hydrated, and to what extent, is an interesting and important point. The thermodynamic analysis does not provide an unambiguous answer to this question, though it is inconsistent with substantial hydration of the transition state. This is because immobilization of water molecules in the transition state would be expected to reduce the activation entropy, whereas the experimentally-determined activation barrier is large and favorable. Because the absolute magnitude of the gain in conformational entropy is experimentally inaccessible, however, the issue of whether the transition state is hydrated, and if so, to what extent, cannot be unequivocally determined. We note that the mutagenesis results, which demonstrate that alterations in the entropy term are usually inversely related to the enthalpic alterations except in the case of W120F, also argue against substantial hydration of the transition state. These results are consistent with a simple mechanistic trade-off between generating greater enthalpic binding interactions at the cost of protein/ligand conformational entropy, or vice versa. The enthalpy and entropy associated with water ordering at protein surfaces are generally considered to be mutually unfavorable, and if our energetic measurements were dominated by this process we would expect changes in the same direction rather than the balancing phenomena we observe. It would thus appear that in the streptavidin−biotin example, the entropy terms for the dissociation process are dominated by the conformational entropy components rather than solvent-related components.

Why is Trp Selected in the High-Affinity Streptavidin−Biotin Complex? The thermodynamic profiles in Figure 4 summarize the energetic mechanisms by which streptavidin utilizes Trp side chains to maximize the activation barrier for biotin dissociation. A general finding is that the Trp side chains clearly optimize the balance between enthalpic benefits and entropic costs in either the ground state or the transition state. This is related to the common phenomenon of enthalpy/entropy compensation,[22] which can be viewed in a descriptive sense as the energetic balance between favorable solvent release and bonding interactions (H bonds, van der Waals, hydrophobic) versus the unfavorable conformational immobilization of the protein and ligand. At position 79, Phe actually increases the ΔH° ($\Delta\Delta H^\circ = -1.5$ kcal^{-1}), but at an even larger entropic cost ($T\Delta S^\circ = -2.4$ kcal^{-1}). There is a severe 5.1 kcal mol^{-1} equilibrium enthalpic cost ($\Delta\Delta H^\circ$) to Phe substitution at position 120, but this is lessened by a favorable $T\Delta S^\circ$ of 2.8 kcal/mol. At position 108, the substitution of Phe for Trp increases the enthalpic activation barrier to dissociation ($\Delta\Delta H_r^\ddagger = +4.5$ kcal mol^{-1}), but at a compensating favorable activation entropy gain ($T\Delta S_r^\ddagger = +6.2$ kcal mol^{-1}), so that the free energy barrier to dissociation is lowered.

In a mechanistic sense, these results are consistent with the need for high-affinity systems to make ground state trade-offs between increasing enthalpically favorable binding interactions and incurring costly increases in protein/ligand immobilization. It is interesting to note that the ground-state free energy alteration of W79F is entropically dominated. This suggests that Trp 79 is particularly suited to control the entropic costs of biotin immobilization. This role correlates well with its interaction site, where Trp 79 is the key contact with the valeric acid tail of biotin, expected to be the most mobile portion of the ligand. The protein thus sacrifices potential benefit arising from a more favorable binding enthalpy, observed with Phe at this position, in order to optimize the enthalpy/entropy balance. The decrease in binding enthalpy is again correlated with an increased entropic benefit, leading to a mechanistic model where the biotin hydrocarbon tail maintains more conformational freedom in the bound state with Trp at position 79 than with Phe. An interesting corollary to this model is seen with Trp 108, where the side chain has been clearly selected to optimize the *transition state* enthalpy/entropy balance. In the streptavidin transition state, the activation barrier is increased when binding interactions are reduced (activation enthalpy increased), but this apparently also results in a corresponding reduction in protein/ligand immobilization, so that the activation entropy becomes substantially more favorable. This balance is optimized with Trp, while W108F displays a reduced activation barrier despite an increased activation enthalpy (weaker transition state binding interactions), due to the dominance of the favorable activation entropy gain that is probably associated with increased protein/ligand mobility.

In summary, the large free energy activation barrier to biotin dissociation that determines the high affinity of the streptavidin−biotin interaction is dominated by a large and positive activation enthalpy, indicating a significant loss of binding contacts between protein and ligand in the transition state and the presence of endothermic conformational alterations. The positive activation entropy change associated with the formation of the transition state is also consistent with significant protein−ligand conformational alterations in the transition state, resulting in a gain in conformational entropy of the system. The mapping of the transition state and ground state energetics for the Trp to Phe mutants has provided preliminary molecular details of the transition state structure. Formation of the transition state results in loss of binding contacts between biotin and Trp 79 and Trp 120, whereas Trp 108 retains substantial binding contact with biotin. We expect that a clearer and higher resolution picture of the transition state complex will develop from further mutagenesis studies of the hydrogen-bonding contacts and of the flexible loop closure associated with biotin binding. These studies should provide a good test of the transition state model generated here, as the hydrogen-bonding contacts in particular are numerous and should more precisely define regions of the binding pocket that maintain interactions with biotin in the transition state. The precise mapping of differences in the thermodynamic parameters to specific molecular parameters such as protein−ligand contact areas,[25] the ordering of surface residues ("local folding"),[26] and larger conformational changes awaits three-dimensional structure determinations and further delineation of the temperature effects on the enthalpy of binding (ΔC_p measurements).

Acknowledgment. We thank Prof. Mark Fisher for assistance with initial calorimetry experiments, Cynthia Long for assistance with the construction of the synthetic core streptavidin gene, Phillip H. Tan and Chuck Sleeth for help with the expression and purification of streptavidin mutants, and Allan S. Hoffman for the use of his laboratories in performing the off-rate experiments. The isothermal titration calorimetry measurements were performed at the Biocalorimetry Center, a Biomedical Research Technology Resource Center sponsored by the National Institutes of Health (RR04328), Johns Hopkins University, Department of Biology, Baltimore, MD. This research was supported in part by the National Science Foundation (BCS9309360), Battelle Pacific Northwest Laboratories, the Whitaker Foundation, and NIH (R01 DK 49655-01).

JA950257A

(25) (a) Freire, E. *Arch. Biochem. Biophys.* **1993**, *303*, 181−184. (b) Murphy, K. P.; Xie, D.; Garcia, K. C.; Amzel, L. M.; Freire, E. *Proteins* **1993**, *15*, 113−120.

(26) Spolar, R. S.; Record, M. T. *Science* **1994**, *263*, 777−783.